Journal of the European Ceramic Society xxx (xxxx) xxx–xxx

Contents lists available at ScienceDirect

Journal of the European Ceramic Society

journal homepage: www.elsevier.com/locate/jeurceramsoc

Original Article

Non-Hall-Petch hardness dependence in ultrafine fibrous $MgAl_2O_4$-MgO eutectic ceramics fabricated by the laser-heated floating zone (LFZ) method

Bibi Malmal Moshtaghioun*, Jose I. Peña

Instituto de Ciencia de Materiales de Aragón, CSIC-Universidad de Zaragoza, campus Río Ebro, 50018, Zaragoza, Spain

ARTICLE INFO

Keywords:
$MgAl_2O_4$-MgO eutectic
Modelling of hardness
Laser float zone

ABSTRACT

$MgAl_2O_4$-MgO eutectic ceramics were fabricated by the laser-heated floating zone (LFZ) method with various growth rates to assess its possible beneficial effect on microstructural aspects and mechanical properties. It was determined that the growth rate optimizing the microstructure and mechanical properties is 750 mm/h; below this value, coarsening of the fibrous microstructure takes place with a degradation of these properties. In the extreme case of 50 mm/h growth rate, the presence of undesirable transverse cracks was unavoidable. Thanks to the high growth rate of 750 mm/h, ultra-fine fibrous microstructure $MgAl_2O_4$-MgO eutectic ceramics can thus be fabricated with greater hardness (15.5 GPa from Vickers indentation and 22 GPa from nanoindentation) and flexural strength (˜345 MPa). It is reported that hardness scales with the interfiber spacing λ according to a law of the type $ln\lambda/\lambda$, contrary to the assumed Hall-Petch-like dependence. This proposed law can be explained in terms of dislocation hardening induced by the MgO fibers.

1. Introduction

Spinel ceramic ($MgAl_2O_4$), and its eutectic with MgO, have been receiving considerable attention within the engineering ceramics community, especially for their use in structural and functional applications requiring ultrafine and dense microstructure [1–7]. The most popular of these applications in the case of this eutectic system is perhaps for photonic devices or catalysts [3]. There is also great motivation within the field in refining the microstructure of $MgAl_2O_4$-MgO eutectic ceramics to the ultrafine range and ideally to the nanoscale [1–3], for mechanical properties improvement [2].

Fortunately, directionally solidified eutectic ceramics grown from melt are found to be fully-dense ceramics with fine and homogeneous microstructure, which present higher potential in mechanical, thermal shock resistance and strength properties. This is due to their strong coherent bonding in their interfaces together with its defect-free nature [8,9]. Previous studies [5–7] suggest that this method certainly appears attainable if the growth rate to fabricate $MgAl_2O_4$-MgO eutectic ceramics is appropriately optimized. However, the fabrication of $MgAl_2O_4$-MgO eutectic ceramics with the ultrafine fibrous microstructure retention and its impact on mechanical properties of this system are still not studied systematically.

With these premises in mind, the objectives of the present study were to grow $MgAl_2O_4$-MgO eutectic ceramics by the laser-heated floating zone (LFZ) method with variable growth rates and evaluate the possible beneficial effect of different growth velocities on their microstructure as well as their hardness and flexural strength, when they are compared with those of conventional spinel ceramics ($MgAl_2O_4$).

2. Experimental procedure

Eutectic rods of a mixture of $MgAl_2O_4$-MgO were grown by directional solidification from the melt using the laser-heated floating zone (LFZ) method with a CO_2 laser [8]. The starting materials were commercially available Al_2O_3 powder (Sigma-Aldrich, 99.99%) and MgO powder (Sigma-Aldrich, > 99%). MgO powder was dried in a furnace at 1200 °C for 6 h to remove the possible moisture absorption from outside air [10]. There is only one eutectic composition between Al_2O_3 and MgO, which appears at 55 wt% Al_2O_3 and 45 wt% MgO and its melting temperature is around 1999 °C [11]. Precursor rods of ˜ 3 mm in diameter and up to 5 cm in length were prepared by cold isostatic pressing for 5 min at 200 MPa followed by pre-sintering in a furnace at 1500 °C for 12 h.

The pre-sintered rods were then grown by LFZ in air, in all cases using two-growth steps of diameter reduction at growth rate of 300 mm/h. The last step, however, was performed with the solidified rod being pulled out downwards using a variable growth rate between 50 and 750 mm/h to evaluate its effect on the densification, average

* Corresponding author at: Instituto de Ciencia de Materiales de Aragón, Universidad de Zaragoza, campus Río Ebro, Zaragoza, Spain.
E-mail addresses: mali@unizar.es, mali_moshtagh@us.es (B.M. Moshtaghioun).

https://doi.org/10.1016/j.jeurceramsoc.2019.04.015
Received 9 January 2019; Received in revised form 2 April 2019; Accepted 7 April 2019
0955-2219/

grain size, hardness, indentation fracture toughness and strength of the resulting $MgAl_2O_4$-MgO eutectic ceramics. A nominal laser output power of 40–50 W has been used in the last step to maintain a constant feed and very small molten zone. All steps were performed in contra-rotation of the crystal and precursor with 50 rpm and eutectic rods of ˜1 mm were fabricated.

Later on, the grown eutectic rods were first cut, ground and polished to a 0.25 μm finish. The one grown at 100 mm/h was analysed by X-ray diffraction (XRD) performed at room temperature using one X-ray diffractometer (Model D-Max Rigaku) operating in the reflexion mode with Cu-Kα radiation in polycrystalline powders of the eutectic sample. Additionally, all were characterized microstructurally by a field emission scanning microscopy (FE-SEM) (model Merlin, Carl Zeiss, Germany) with an EDS microanalysis system INCA350 from Oxford Instruments. Microstructure observations were done from both transverse and longitudinal sections using the back-scattered emission (BE) mode on carbon coated-polished surfaces. The phase interspacing, λ, was determined from the transverse cross-section SEM micrographs.

Furthermore, mechanical properties were studied by Vickers-indentation tests (Matsuzawa MXT70 micro-hardness tester) applying a load of 9.81 N for 15 s on cross-sections of eutectic rods to evaluate Vickers hardness [12,13]. Nanoindentation tests (Agilent Technologies G200, U.S.A. equipped with a Berkovich indentor) at 250 mN with constant loading rate of 0.5 mN/s were done as well, to measure hardness and elastic modulus from loading-unloading curves. Finally the strength of rods in longitudinal direction was measured by flexural tests carried out in a three-point bending test fixture of 10 mm loading span in Instron testing machine (Instron 5565). The tests were performed at constant crossheads speed of 0.05 mm/min.

3. Results and discussion

The crystal structure of the eutectic components was determined by XRD. Fig. 1 shows the XRD pattern of crushed eutectic crystal grown at 100 mm/h of solidification rate. The crystalline $MgAl_2O_4$ (spinel) and MgO (periclase) were detected as main phases which confirms the complete eutectic formation during crystal growth. Apart from that, there is a trace of contamination of alumina phase because of crushing in alumina mortar.

The microstructure of the $MgAl_2O_4$-MgO eutectics was studied using FE-SEM. The presence of tiny pores was observed in the interior of the eutectic rods grown at any growth rate, whereas those grown at a growth rate lower than 100 mm/h contained large transverse cracks. Fig. 2 compares representative transverse cross section FE-SEM images of the $MgAl_2O_4$-MgO eutectic ceramics grown at different velocities. A fibrous microstructure which corresponds to the minority phase volume

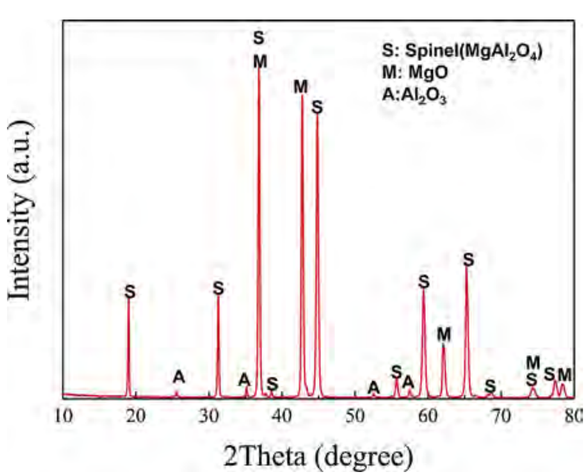

Fig. 1. XRD patterns of crushed $MgAl_2O_4$-MgO eutectic crystal grown at 100 mm/h of growth rate.

fraction of 24.51% was observed (Fig. 2). This fact is in agreement with the general behaviour of binary eutectics where a cross-over from fibrous to lamellar patterns is predicted at volume fractions of the minority phase above approximately 0.287 [14]. By EDS analysis, the bright matrix was detected to be spinel and the small and dark embedded phases were MgO. At low growth rate of 50 mm/h, irregular MgO fibrous microstructure in a spinel matrix was observed (Fig. 2(A)). As it is expected for directional solidification of eutectic ceramics, the microstructure is strongly dependent on the growth rate. The higher growth rate, the finer the microstructure and at a growth rate of 100 mm/h, some inhomogeneity in the microstructure was observed that can be related to the beginning of colonies formation (Fig. 2(B)). It means that finer dispersed MgO fibers embedded in a spinel matrix with some evidence of coarse irregular MgO grains and $MgAl_2O_4$ matrix inter-structure was observed. For growth rate of 300 and 750 mm/h, the presence of a colony microstructure was distinguished especially in the centre of solidified rods (Fig. 2 C and D) consisting of ultrafine dispersed MgO fibers inside the colonies and these ones were surrounded by an irregular structure of coarsened MgO and spinel phases. In the case of 750 mm/h growth rate, the colonies were well framed with almost equiaxial shape in the transverse cross section with a diameter about 25 μm and presented a boundary of ˜5 μm in thickness. While for 300 mm/h growth rate, microstructure was consisted of more irregular colonial and inter-colonial structure made it difficult to estimate the size of colonies and the inter-colony space.

Fig. 3 shows higher magnification of the microstructure in transverse and longitudinal sections of grown rods with the rate of 750 mm/h and 50 mm/h. In the case of 750 mm/h growth rate inside the colonies, an ultra-fine (sub-micrometric) eutectic microstructure was obtained in which the MgO fibers seem to be mainly triangular in cross section with size of 100–200 nm (Fig. 3(A)) and be short in their length (Fig. 3(B)); however it is probable that they pass in and out of the polishing surface and the real length can be higher. In the case of 50 mm/h growth rate, the cross-section of the fibers is more irregular (Fig. 3(C)) and frequently joined fibers with larger cross-sections (Fig. 3(C, inset) with size of ˜300– 1500 nm was observed. In longitudinal cross-section, MgO fibers are to some extent longer than in the case of 750 mm/h (Fig. 3(D)). The presence of transverse cracks in the rods grown at lower rate is related to a thermal expansion mismatch and the high aspect ratio of this growth rate; a similar feature was reported previously [5,6]. When the MgO fibers reduced to sub-micrometric size and shorter in length at higher growth rate, the fabricated rods are free from transverse cracks. It seems that there is a critical aspect ratio for the formation of transverse cracks that happened at growth rate ≤50 mm/h with ˜1 mm in final diameter. Microstructural evaluation with growth rate was also studied by measuring the interspacing (λ) of MgO fibers estimated by transverse SEM micrographs as a function of the growth rate (Table 1). The data are fitted to the Hunt-Jackson typical quadratic law of $\lambda = cV^{-1/2}$ where c is constant and in this case is equal to 5.2 (Fig. 4).

With respect to mechanical properties, the first assessment was done by Vickers indentation to estimate the hardness of $MgAl_2O_4$-MgO eutectic rods grown at variable velocities and the results are listed in Table 1. Hardness values are independent of the indentation direction meaning that similar values were obtained from transverse and longitudinal sections. An increase of hardness with the decrease of interfiber spacing was observed, which reaches values up to 15.5 GPa for eutectic ceramic grown at 750 mm/h growth rate. Contrary to what it is commonly reported [15], the interfiber spacing dependence (λ) of the hardness does not fit into a Hall-Petch (i.e. a $\lambda^{-1/2}$) law if we keep strictly rigorous in the accuracy of the fitting (regression factor is lower than 0.9). A much more accurate fitting is achieved assuming an almost linear dependence of the hardness with the inverse of the interspacing (i.e. a λ^{-1}) law. (Regression factor r = 0.95).

A plausible explanation for this is based on the following picture: the fibers are likely to be obstacles for dislocation motion, as suggested

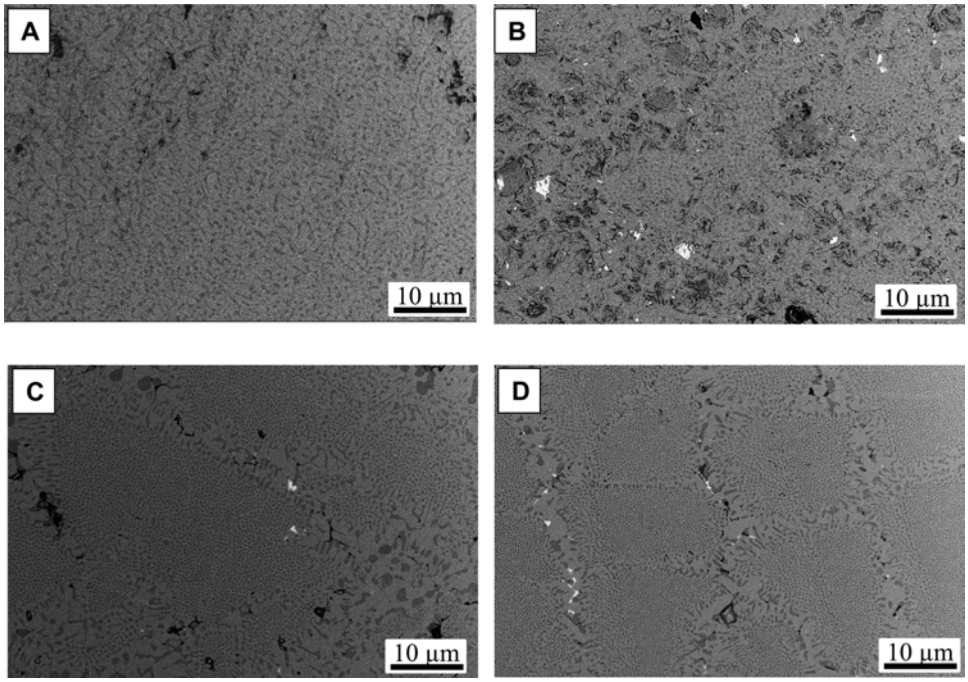

Fig. 2. Representative FE-SEM micrographs of $MgAl_2O_4$-MgO eutectic crystal in transverse section grown at (A) 50, (B) 100, (C) 300 and (D) 750 mm/h.

elsewhere [16]. It is reported that low-temperature plasticity in $MgAl_2O_4$ is controlled by dislocation glide along (111) planes with Burgers vectors b = a/4[1 $\bar{1}$ 0] type and eventually cross-slip along [100] direction [17]. The threshold stress for dislocation motion is the sum of the intrinsic friction stress for dislocation motion in the pure $MgAl_2O_4$ phase (σ_0) plus the stress due to the line tension of the curved dislocations confined in a typical mean distance *l*. The value of the line tension stress is provided in Ref. [18] (see equation (3) in that reference) and it is given by $\frac{Gb}{2\pi(1-\upsilon)l}\left[\ln\left(\frac{l}{b}\right)+1\right]=\frac{Gb}{2\pi(1-\upsilon)l}\ln\left(e\frac{l}{b}\right)$ where *G* is the shear modulus of that phase, *b* the modulus of the Burgers vector, υ the Poisson's modulus, *l* the mean distance between dislocations and $e=\lim_{n\to\infty}(1+1/n)^n\cong 2.7182\ldots$ [18]. The dislocation mean distance is related to the interfiber spacing in the following one: From one side, the dislocation microstructure must follow the forest hardening relationship, i.e. $\tau=\alpha Gb\sqrt{\rho}=\alpha Gb/l$ where α≅0.3. On the other side, the presence of fiber arrays with a periodicity of λ induces a dislocation patterning with that spatial period. Such pattern must follow the principle of similitude, i.e. $\frac{\tau}{G}=K\frac{b}{\lambda}$, because the material

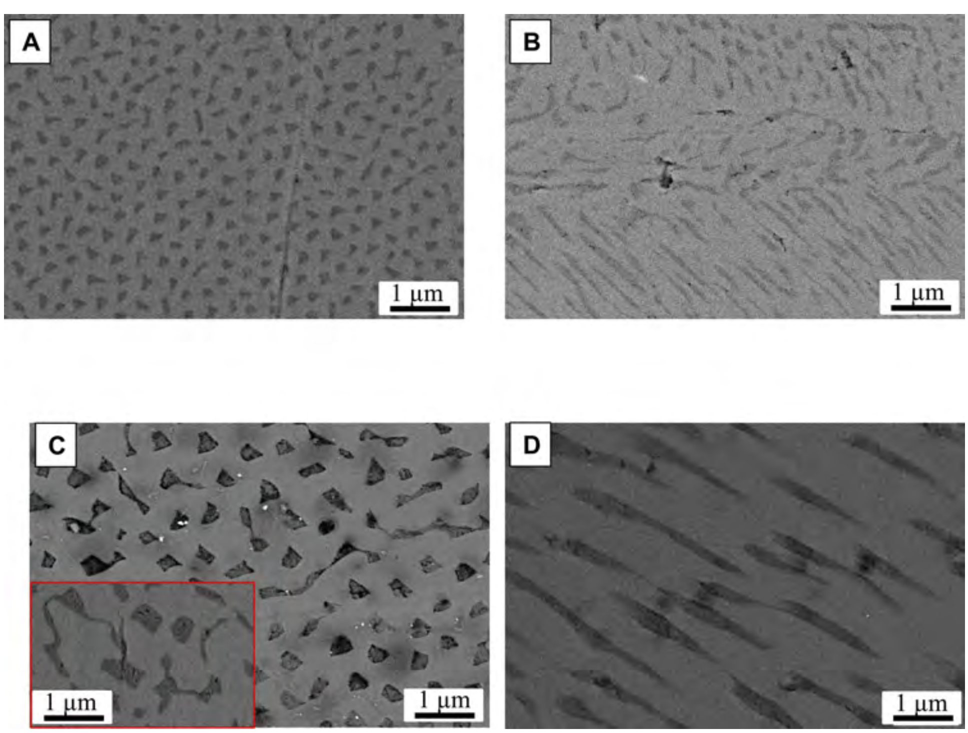

Fig. 3. Microstructure of $MgAl_2O_4$-MgO eutectic crystal with higher magnification grown at (A) 750 mm/h from transverse section, (B) 750 mm/h from longitudinal section, (C) 50 mm/h from transverse section, inset shows irregular joined fibers and (D) 50 mm/h from longitudinal section.

Table 1
Growth rates, microstructural features and Vickers hardness of $MgAl_2O_4$-MgO eutectic ceramics prepared in this study.

Growth rate (mm/h)	Interfiber spacing (µm)	Hardness by Vickers indentor 9.81 N (HV1) (GPa)	
		Trans.	Long.
50	1.059 ± 0.107	14.1 ± 0.2	14.1 ± 0.5
100	0.952 ± 0.099	14.3 ± 0.3	14.5 ± 0.1
300	0.738 ± 0.076	14.5 ± 0.3	14.5 ± 0.2
750	0.534 ± 0.059	15.5 ± 0.4	15.7 ± 0.3

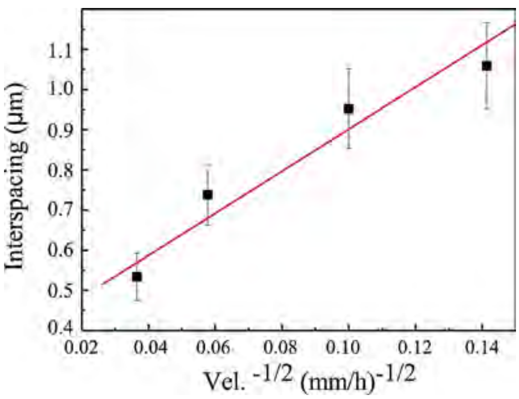

Fig. 4. Interfiber spacing versus inverse square root of growth rate.

satisfies all the conditions for patterning formation, where K≅10 in most materials. A thorough discussion on patterning formation and the principle of similitude is given in [19]. Combining these two equations, it yields $l = \frac{\alpha}{K}\lambda = f\lambda$, where f≅0.03. Finally, introducing the spacing λ into the line tension expression, it is possible to write:

$$\sigma = \sigma_0 + \frac{Gb}{2\pi(1-\nu)f\lambda}\ln(fe\frac{\lambda}{b}) \tag{1}$$

As commented previously, the symbols G and υ stands for the shear and Poisson's moduli of $MgAl_2O_4$ respectively and their values are G≅96 GPa and υ≅0.27) [20].

Fig. 5 displays the experimental values of hardness from transverse section versus the inverse of interfiber spacing. The solid one is the function provided in Eq. (1). The agreement is satisfactory (r = 0.996) and gives a support to this interpretation, although the final proof will certainly require a TEM microscopy study of the dislocation microstructure in deformed specimens. Some reports in literature seem to validate this interpretation, because pieces of evidence of dislocation activity have been detected in nanostructured transparent $MgAl_2O_4$ ceramics after nanoindentation testing [21]. At this regard, doubts arise for the validity of the classical Hall-Petch has been pointed out by other authors in the case of the B_4C-TiB_2 laser-processed eutectic ceramics (a linear scaling is more appropriate in their case) but no explanation to this is given [22].

To our knowledge, there are some reasons which may justify the possible non-validity of the Hall-Petch law: first, the least-square method does not provide a clear improvement of the fitting for a $\lambda^{-1/2}$ scaling. Second, MgO fibers are not as strong as grain boundaries for dislocation blocking and they do not behave as sinks or sources for them. Most models developed for explaining Hall-Petch law make use of either dislocation pile-ups induced by grain-boundary blocking or they rely on the kinetics of grain-boundary dislocation sources. None of these is present in our system.

Quite recently, Li et al. [23] have published a remarkable criticism of the validity of the Hall-Petch law. Their main conclusions can be summarized as follows: the choice of that law is many times a question

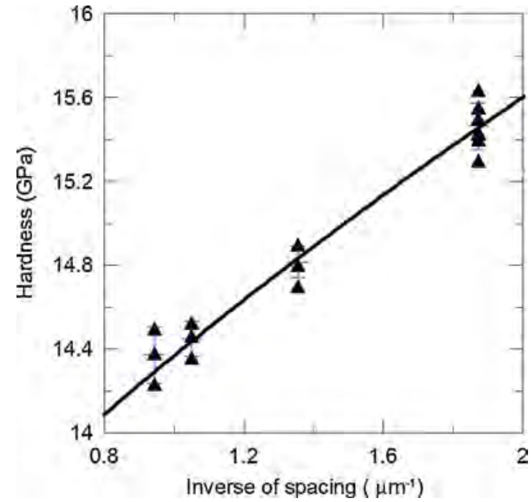

Fig. 5. Hardness from transverse section versus the inverse of spacing for $MgAl_2O_4$-MgO eutectic ceramics considered in this study. The solid line is the function provided in Eq. (1) in the text. Data points displayed for each specimen are those which are inside the interval [X_M-σ, X_M+σ], where X_M is the mean value of all data for a given sample and $w = \sum_i (X_i - X_M)^2/N$. The number of data for each sample was N = 10.

of convenience and most experimentalists are familiar with it and they abandon any possible alternative law if the fitting seems to be minimally reasonable. It is also a consequence of inertial effects in research: Hall-Petch-type behaviour is the "normal" tendency and none of the authors nor the reviewers would be surprised if this law is invoked. Remarkably, a Bayesian analysis of several sets of experimental data carried out by Li et al. [23] prove that in most cases either $\lambda^{-1/2}$ or λ^{-1} are acceptable: they are not distinguishable from a statistically point of view. The most accurate law is of the type *ln*λ/λ, and this is the reason why either $\lambda^{-1/2}$ or λ^{-1} dependences are considered in literature. Since a law of the form *ln*λ/λ is a well-founded one in the frame of the theory of plasticity and dislocation theory, this latter one should be preferable. In the case of our system, in which none of the usual assumptions justifying a Hall-Petch law is present, the option of a forest hardening law scaled with the mean spacing of fibers seem to be more natural and the fitting with data is consistent with the well-based law commented above. In any case, the experimental agreement is quite reasonable after all.

The hardness of the grown eutectic bars in all cases is higher than both components of this eutectic. More specifically, reported values of micro-hardness for MgO are about 5–8 GPa [24] and for $MgAl_2O_4$ is ˜13.5 GPa [2], which confirms the hardness improvement of $MgAl_2O_4$-MgO eutectic system as a result of the reduction in the spacing of the MgO fibers to sub-micrometric fibrous structure. Furthermore, it is found that precipitation hardening of MgO and $MgAl_2O_4$ is possible [6] according to the phase diagram and may intensify the hardening effect of interfiber spacing, as well.

The finest eutectic structure rods grown with 300 and 750 mm/h growth rate were objected for further mechanical tests to measure hardness and elastic modulus by nanoindentation and flexural strength by three-point bending tests. The results are collected in Table 2. Hardness measured by a nanoindentation is usually higher than micro-hardness by Vickers from the same rods (Table 2). This can be associated with the fact that microindentation is more sensitive to microstructural defects like pores and micro-cracks which are intrinsically inside the grown rods or created by micro-hardness measurement. However, the values of hardness from nanoindentation are similar in both transverse and longitudinal sections and the same trend of improved hardness with growth rate was observed which reached to ˜22 GPa for eutectic ceramics grown at 750 mm/h growth rate.

Table 2
Mechanical response by nanoindentation and three-point bending tests of selected $MgAl_2O_4$-MgO eutectic ceramics.

Growth rate (mm/h)	Interfiber spacing (μm)	Hardness by nano-indentor with load of 250 mN (GPa)		Elastic modulus by nano-indentor with load of 250 mN (GPa)		Flexural strength (MPa)
		Trans.	Long.	Trans.	Long.	
300	0.738 ± 0.076	18.2 ± 1	18.9 ± 1	299.5 ± 25	298.3 ± 27	241.8 ± 54
750	0.534 ± 0.059	22.1 ± 1	22.7 ± 1	308.7 ± 30	313.9 ± 25	343.7 ± 38

Regarding elastic modulus, the value is ˜ 300 GPa independent of solidification rate from 300 to 750 mm/h and direction of measurement (transverse or longitudinal sections), although a narrow scatter is unavoidable. This behaviour is expected because the volume fractions of the phases are the same for all growth rates and elastic modulus value is the representative of the matrix-fiber bonding magnitude. This value is comparable with elastic modulus data of 290 GPa and 300 GPa reported for $MgAl_2O_4$ and MgO, respectively [3,25].

Finally, three-point bending tests were performed to go into the flexural strength behaviour. It was assumed a cylindrical geometry and the flexural strength (σ_f) was calculated according to the classical expression $\sigma_f = FL/\pi R^3$, where F is the load applied at the centre of the beam, L is the support span and R is the radius of the beam. The results are listed in Table 2. An increment of strength with the growth rate was observed, ranging from 242 to 344 MPa. No plasticity was observed. Enhanced strength was obtained at higher growth rate and it reached ˜345 MPa at 750 mm/h, while the strength value for the $MgAl_2O_4$ matrix is around 150–200 MPa [3,4]. This can be explained as a result of a reduction in the spacing of the MgO fibers by a factor 0.7 which improved the strength inversely with the fiber spacing (factor ˜1.4). This is in good agreement with the behaviour of other eutectic ceramics [26].

4. Conclusions

It is convenient to mention explicitly that $MgAl_2O_4$-MgO eutectic rods with ultrafine fibrous microstructure and enhanced mechanical properties can readily be fabricated by laser-heated floating zone (LFZ) method. Based on the experimental results and analyses, the following conclusions can be drawn:

1 LFZ method is an effective and affordable method for the $MgAl_2O_4$-MgO eutectic ceramics and is therefore very appealing for optimizing the microstructure and consequently the mechanical properties by controlling the growth rate.
2 $MgAl_2O_4$-MgO eutectic ceramics can be optimally grown at 750 mm/h, resulting in ultra-fine fibrous eutectic ceramics free from transverse cracks. Lower growth rate below 750 mm/h causes coarsening the fiber interspacing which is detrimental for the mechanical properties and catastrophic decrement happens for 50 mm/h growth rate with the presence of transverse cracks.
3 Regarding mechanical properties, $MgAl_2O_4$-MgO eutectic ceramics fabricated at 750 mm/h growth rate favourably showed elevated hardness (15.5 GPa from Vickers indentation and 22 GPa from nanoindentation) and strength (˜345 MPa) compared with spinel matrix.
4 One essential feature is the fact that the hardness exhibits an almost linear dependence with the fibers spacing, rigorously a dependence of the form $ln\lambda/\lambda$. Such law is not commonly used in the literature of eutectic ceramics but it is experimentally based on the better accuracy and also is supported by recent theoretical considerations on the excessive use of the Hall-Petch dependence when the microstructure is far from being compatible with the assumptions made for the formulation of this law.

Acknowledgements

This work was supported by the Ministerio de Economía y Competitividad (Government of Spain) and FEDER Funds under Grants No. MAT2016-77769-R BMM wants to acknowledge the support of the Spanish MINECO by means of a “Juan de la Cierva-Incorporación” fellowship during her sabbatical stay in Zaragoza.

References

[1] A.F. Dericioglu, A.R. Boccaccini, I. Dlouhy, Y. Kagawa, Effect of chemical composition on the optical properties and fracture toughness of transparent magnesium aluminate spinel ceramics, Mater, Trans. 46 (2005) 996.
[2] A. Krell, A. Bales, Grain size- dependent hardness of transparent magnesium aluminate spinel, Int. J. Appl. Ceram. Technol. 8 (5) (2011) 1108.
[3] A. Goldstein, A. Goldenberg, M. Vulfson, Development of a technology for the obtainment of fine grain size, transparent $MgAl_2O_4$ spinel parts, J. Ceram. Sci. Tech. 2 (2011) 1.
[4] O. Tokariev, T. Van Gestel, M. Bram, J. Malzbender, Strength enhancement of transparent spinel ceramics, Mater. Lett. 107 (2013) 364.
[5] F.L. Kennard, R.C. Bradt, V.S. Stubican, Eutectic solidification of MgO-$MgAl_2O_4$, J. Am. Ceram. Soc. 56 (1973) 566.
[6] F.L. Kennard, R.C. Bradt, V.S. Stubican, Mechanical properties of the directionally solidified MgO-$MgAl_2O_4$ eutectic, J. Am. Ceram. Soc. 59 (1976) 160.
[7] J.H. Lee, A. Yoshikawa, T. Fukuda, Growth of MgO/$MgAl_2O_4$ eutectic crystals by the micro-pulling-down method and its characterization, J. Eur. Ceram. Soc. 25 (2005) 1351.
[8] J. LLurca, V.M. Orera, Directionally solidified eutectic ceramic oxide, Prog. Mater. Sci. 51 (2006) 711.
[9] V.S. Stubican, R.C. Bradt, Eutectic solidification in ceramic systems, Annu. Rev. Mater. Sci. 11 (1981) 267.
[10] C. Rode, T. Bunch-Nielsen, K.K. Hansen, B. Grelk, Moisture damage with magnesium oxide boards in Danish façade structures, Energy. Proc. 132 (2017) 765.
[11] A.M. Alper, R.N. Mcnally, P.H. Ribbe, R.C. Doman, The system MgO-$MgAl_2O_4$, J. Am. Ceram. Soc. 45 (1968) 263.
[12] D.J. Green, An Introduction to the Mechanical Properties of Ceramics, Cambridge University Press, Cambridge, UK, 1998.
[13] G.R. Anstis, P. Chantikul, D.B. Marshall, B.R. Lawn, A critical evaluation of indentation techniques for measuring fracture toughness: I direct crack measurements, J. Am. Ceram. Soc. 64 (1981) 533.
[14] V.M. Orera, J.I. Peña, Directional Solidification in Ceramics and Composites: Processing Methods, John Wiley & Sons, Inc., Hoboken, New Jersey, 2012, p. 417.
[15] R.W. Rice, C.C. Wu, F. Borchelt, Hardness-grain size relation in ceramics, J. Am. Ceram. Soc. 77 (1994) 2539.
[16] J. Llorca, V.M. Orera, Directionally solidified eutectic ceramic oxides, Prog. Mater. Sci. 51 (2006) 711.
[17] P. Veyssière, C.B. Carter, Dissociation of dislocations in $MgAl_2O_4$ spinel deformed at low temperatures, Phil. Mag. Lett. 57 (1988) 211.
[18] D. Gómez-García, B. Devincre, L.P. Kubin, Dislocation dynamics in confined geometry, J. Comp-Aid Mater. Des. 6 (1999) 157.
[19] D. Gómez-García, B. Devincre, L.P. Kubin, Dislocation patterns and the similitude principle: 2.5D mesoscale simulations, Phys. Rev. Lett. 96 (2006) 125503.
[20] https://Materials project.org/materials/mp-3536/.
[21] J. Zhang, T. Lu, X. Chang, N. Wei, J. Qi, Unique mechanical properties of nanostructured transparent $MgAl_2O_4$ ceramics, Nanoscale Res. Lett. 8 (2013) 261.
[22] R.M. White, J.M. Kunkle, A.V. Polotai, E.C. Dickey, Microstructure and hardness scaling in laser-processed B_4C-TiB_2 eutectic ceramics, J. Eur. Ceram. Soc. 31 (2011) 1227.
[23] Y. Li, A.J. Bushby, D.J. Dunstan, The Hall–Petch effect as a manifestation of the general size effect, Proc. R. Soc. A472 (2016) 20150890.
[24] F. Giberteau, A. Dominguez-Rodriguez, R. Márquez, J. Castaing, Deformation of MgO by Vickers microindentation tests, Revue de Physique Apliquée 17 (1982) 777.
[25] H. Landolt, R. Börnstein, Magnesium oxide (MgO) Young´s, shear and bulk moduli, poisson´s ratio, II-VI and I-VII compounds; Semimagnetic compounds, Part of the Londolt- Börnstein-group III Condensed Matter Book Series, Vol 41B (1970–2017).
[26] C.O. Hulse, J.A. Batt, Effect of eutectic microstructures on the mechanical properties of ceramic oxides, Tech. Rept. L-910803-7, (1974).